

AD A 030749 SPD-479-13

NOTES OF THE DESIGN OF TWO SUPERCAVITATING HYDROFOILS



# DAVID W. TAYLOR NAVAL SHIP RESEARCH AND DEVELOPMENT CENTER

Bethesda, Md. 20084

NOTES OF THE DESIGN OF  
TWO SUPERCAVITATING HYDROFOILS

by

Elwyn S. Baker

APPROVED FOR PUBLIC RELEASE: DISTRIBUTION UNLIMITED

SHIP PERFORMANCE DEPARTMENT

DDC

RECEIVED

OCT 15 1976

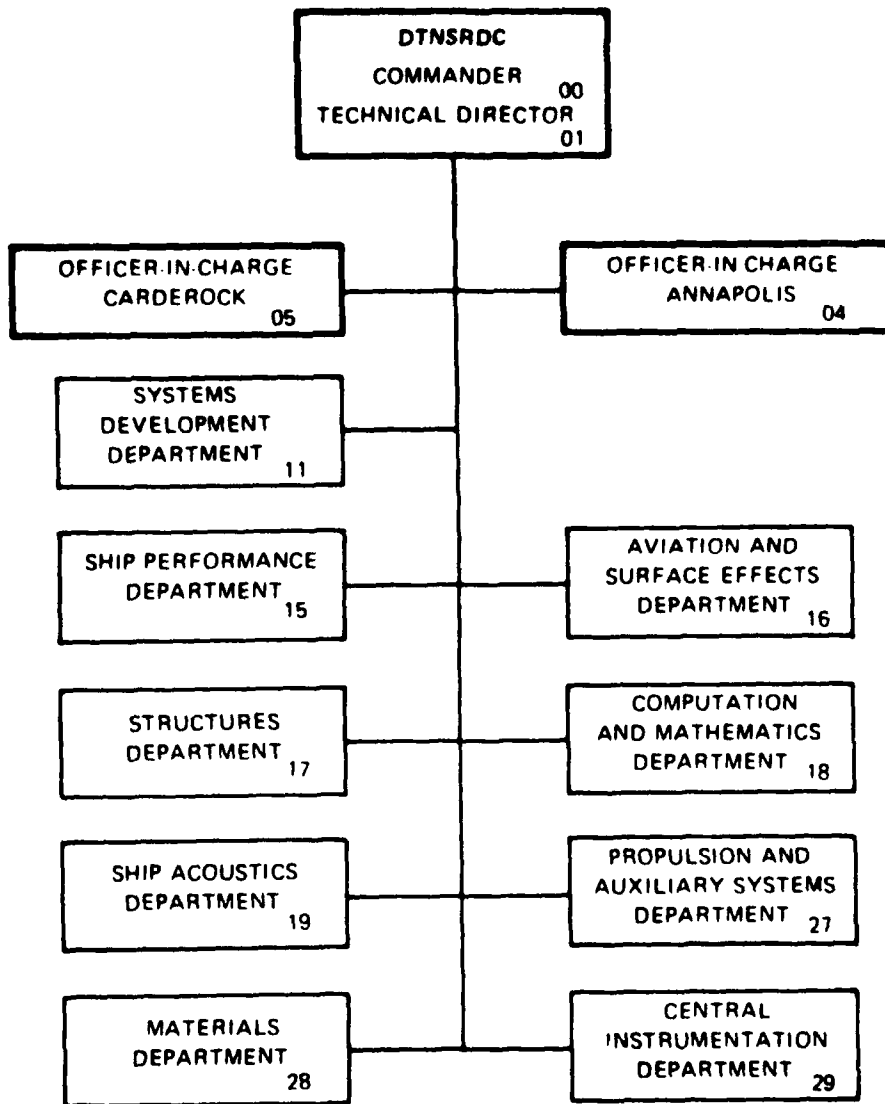
*Handwritten signature*

July 1975

SPD-479-13

12

**MAJOR DTNSRDC ORGANIZATIONAL COMPONENTS**



SECURITY CLASSIFICATION OF THIS PAGE (When Data Entered)

| REPORT DOCUMENTATION PAGE  |  | READ INSTRUCTIONS<br>BEFORE COMPLETING FORM   |
|--|--|---|
| 1. REPORT NUMBER<br>SPD-479-13   | 2. GOVT ACCESSION NO.                      | 3. RECIPIENT'S CATALOG NUMBER   |
| 4. TITLE (and Subtitle)<br>NOTES OF THE DESIGN OF TWO SUPERCAVITATING HYDROFOILS   | 5. TYPE OF REPORT & PERIOD COVERED         | 6. PERFORMING ORG. REPORT NUMBER<br>ZF43-421-001  |
| 7. AUTHOR(s)<br>Elwyn S./Baker   | 8. CONTRACT OR GRANT NUMBER(s)<br>ZF43-421 | 9. PROGRAM ELEMENT, PROJECT, TASK AREA & WORK UNIT NUMBERS<br>62754N Program Element<br>ZF 43421001 Task Area |
| 10. CONTROLLING OFFICE NAME AND ADDRESS<br>David W. Taylor Naval Ship R&D Center<br>Bethesda, Md. 20084  | 11. REPORT DATE<br>Jul 75                  | 12. NUMBER OF PAGES<br>37   |
| 13. MONITORING AGENCY NAME & ADDRESS (if different from Controlling Office)  | 14. SECURITY CLASS. (of this report)       | 15. DECLASSIFICATION/DOWNGRADING SCHEDULE   |
| 16. DISTRIBUTION STATEMENT (of this Report)<br>APPROVED FOR PUBLIC RELEASE: DISTRIBUTION UNLIMITED   |  |   |
| 17. DISTRIBUTION STATEMENT (of the abstract entered in Block 20, if different from Report)   |  |   |
| 18. SUPPLEMENTARY NOTES  |  |   |
| 19. KEY WORDS (Continue on reverse side if necessary and identify by block number)<br>TAP-1, TAP-2, takeoff capability, spanwise twist distribution  |  |   |
| 20. ABSTRACT (Continue on reverse side if necessary and identify by block number)<br>The general design method and some details are discussed for two supercavitating hydrofoil models, TAP-1 and TAP-2. Model design features include takeoff capability and spanwise twist distribution. |  |   |

DD FORM 1473  
1 JAN 73

EDITION OF 1 NOV 68 IS OBSOLETE  
S/N 0102-014-6601

389 694  
SECURITY CLASSIFICATION OF THIS PAGE (When Data Entered)

## TABLE OF CONTENTS

|   | Page |
|---|------|
| ABSTRACT.....                                   | 1    |
| ADMINISTRATIVE INFORMATION.....                 | 1    |
| INTRODUCTION.....                               | 1    |
| SECTION SHAPE SELECTION.....                    | 2    |
| THE DESIGN OF TAP-1 AND TAP-2.....              | 5    |
| PLANNING FOR A TEST PROGRAM.....                | 14   |
| POSSIBLE IMPROVEMENTS TO THE DESIGN METHOD..... | 16   |
| DESIGN OF VENTILATION DOORS.....                | 18   |
| FOIL PERFORMANCE PREDICTION - TAP-1.....        | 20   |
| TAKEOFF PERFORMANCE.....                        | 21   |
| REFERENCES.....                                 | 22   |

## LIST OF TABLES

|  |    |
|--|----|
| Table 1 - Comparison of Numerical Characteristics..... | 25 |
| Table 2 - Section Offsets.....                         | 28 |
| Table 3 - TAP-1.....                                   | 29 |
| Table 4 - TAP-2.....                                   | 30 |

## LIST OF FIGURES

|   |    |
|---|----|
| Figure 1A - Comparison of Foil Sections.....          | 31 |
| Figure 1B - Comparison of Foil Sections.....          | 32 |
| Figure 2 - Comparison of Plan Forms.....              | 33 |
| Figure 3 - Definition of Twist Axis.....              | 34 |
| Figure 4 -- Spanwise Twist Angles.....                | 35 |
| Figure 5 - Strut Spray Wedges and Boundary Layer..... | 36 |

## NOMENCLATURE

| Symbol          | Description   | Dimensions       |
|-----------------|---|------------------|
| $A_1, A_2$      | Angle distribution multipliers in Levi-Civita Program                               | radians          |
| AR              | Aspect ratio  |                  |
| $C_L$           | Lift coefficient, based on foil chordlength and upstream speed                      |                  |
| $C_M$           | Pitching moment coefficient about leading edge                                      |                  |
| $I_{XX}$        | Section moment of inertia about centroid, normalized on fourth power of chordlength |                  |
| L/D             | Ratio of lift to drag force   |                  |
| M               | Bending moment  | F X L            |
| N.A.            | Neutral axis  |                  |
| $S_b$           | Main bending stress (spanwise)  | F/L <sup>2</sup> |
| U               | Upstream speed  | L/T              |
| b               | Span  | L                |
| c               | Chordlength   | L                |
| $c_t$           | Fiber distance from neutral axis to outer surface of material                       | L                |
| d               | Depth   | L                |
| K               | General constant; parameter in Larock and Street's computer program                 |                  |
| t               | Thickness   | L                |
| $t_b, t_1, t_2$ | Parameters in Larock and Street's program   |                  |
| W               | Strut spray wedge angle, degrees  |                  |
| X               | Chordwise distance  | L                |
| Z               | Section modulus   | L <sup>3</sup>   |
| $\bar{Z}$       | Normalized section modulus, based on third power of chordlength                     |                  |

| Symbol      | Description   | Dimensions                      |
|-------------|---|---------------------------------|
| $\alpha$    | Nose-tail line angle of attack                                    | radian                          |
| $\beta$     | Constant angle in Levi-Civita program                             | radian                          |
| $\delta$    | Linearized angle of attack superposed                             | degrees                         |
| $\epsilon$  | Wu's 1955 program parameter related to cavitation number          |                                 |
| $\kappa$    | Linearized camber parameter                                       |                                 |
| $\lambda_i$ | Parameters in Larock and Street's program                         |                                 |
| $\rho$      | Fluid density   | FT <sup>2</sup> /L <sup>4</sup> |
| $\sigma$    | Cavitation number based on cavity pressure                        |                                 |
| $\sigma_v$  | Cavitation number based on vapor pressure                         |                                 |
| $\tau$      | Taper ratio, tip chord/root chord; superposed parabolic thickness |                                 |
| "           | Inches  | L                               |

|               |   |
|---------------|---|
| ACCESSION for |   |
| DTIS          | Write Section <input checked="" type="checkbox"/> |
| DDC           | Diff Section <input type="checkbox"/>             |
| UNANNOUNCED   | <input type="checkbox"/>                          |
| JUSTIFICATION |   |
| BY            |   |
| DATE          | PRIORITY CODES                                    |
| TO            | SPECIAL   |
| A             |   |

D D C  
**RECEIVED**  
OCT 15 1978  
**LIBRARY**  
D

## ABSTRACT

The general design method and some details are discussed for two supercavitating hydrofoil models, TAP-1 and TAP-2. Model design features include takeoff capability and spanwise twist distribution.

## ADMINISTRATIVE INFORMATION

This work was supported by the Naval Material Command under Program Element 62754N, Task Area ZF 43421001, known as the High Speed Struts and Foils Direct Laboratory Funded Project.

## INTRODUCTION

Two supercavitating hydrofoil models have been designed, in an attempt to satisfy the following criteria:

- a. Cruise speed - 80 knots (135 fps)
- b. Static stress not to exceed 20 ksi at cruise, or 45 ksi at maximum load
- c. Cruise lift-to-drag ratio greater than 5.5
- d. Foil system must be able to take off at 35 knots (60 fps)
- e. Lift control available to double or zero lift
- f. Design depth one chord

The general philosophy used here has been to select a two-dimensional section shape, for which design theory and techniques are available, which will satisfy the criteria as closely as possible. Then corrections have been made to the design to account for three-dimensional and boundary effects; for which theory is considerably weaker, using a method similar to strip theory.

Of the two models, the one called TAP-1 is designed to operate in the fully ventilated condition, while TAP-2 should be able to operate with a natural cavity (supercavitating). No base-ventilated foils were considered for these designs.

#### SECTION SHAPE SELECTION

Because the final design wings were to be twisted in the spanwise direction to account for three-dimensional effects, it was thought that the section lift coefficient would approximate the final model lift coefficient rather closely.

The section shape selection for these two foil models was rather difficult because of the takeoff requirement. Presumably the foils would be operating very deep at takeoff and in the supercavitating condition. Because of the high angle of attack and large flap angle required to generate lift at takeoff speed, it was presumed that the natural cavity even at  $\sigma = 0.6$ ,  $C_L \approx 0.80$ , would be long enough to clear the top of the foil model plus a possible 30 percent annex. A takeoff test was planned to measure the takeoff lift to drag ratio for various combinations of angle of attack and flap angle. Because aspect ratio is more important than section shape for generating lift at large incidence angles, it was decided that the two models would have two different aspect ratios, the lower aspect ratio going to the ventilated foil model TAP-1 for which air distribution from the strut might be a problem.

Based on previous experiments<sup>1,2</sup> it was thought that a value  $C_L \approx 0.80$  might be the maximum readily attainable at the takeoff speed. The definition of lift coefficient and the ratio of cruise speed to takeoff speed leads to a factor of 5.22 relating cruise lift coefficient to takeoff lift coefficient, so that the maximum possible design lift coefficient for both foils would be  $C_L \approx 0.15$ .



This is quite a low value of lift coefficient for typical supercavitating hydrofoils. For instance, a flat plate hydrofoil section at  $\sigma = 0$  and  $\alpha = 5^\circ$  produces  $C_L = 0.13$ . Low values of lift coefficient make the design of supercavitating sections difficult for two reasons: first, that the cavity length depends in large part on the fluid deflection, hence lift; and second, because for a separated flow the drag is closely related to the section thickness, whose minimum is governed by structural considerations. It therefore becomes advantageous to the lift-to-drag ratio to generate as much lift as possible with a given thickness, especially when the nonlinear effect of increasing section modulus and bending resistance with thickness is considered. Supercavitating sections with high values of L/D generally have high lift coefficients ( $C_L \sim 0.4$ ) and thin leading edges.

Several major computer programs are available to NSRDC for the design of supercavitating section shapes in infinite fluid medium. One of these, called Wu's 1955 program, is well adapted for low cavitation numbers and was used to design the TAP-1 section. The other, called Larock and Street's program, is better adapted to flows at moderate cavitation number, and was used to design the TAP-2 foil section. Both programs involve a nonlinear computation of cambered foil section properties in infinite stream medium.

In the case when  $\sigma \sim 0$ , such as for a fully ventilated flow, the Wu's 1955 method computer program reduces to the classical Levi-Civita method for cambered hydrofoils in infinite cavity flow, and no wake model is required. Because published theoretical work<sup>3</sup> on the two term section and in-house research showed that a forward center of pressure is desirable to have a high section L/D, it was decided to use essentially a two-term camber shape for the TAP-1 section. However, only a small amount of two-term camber could be added to the basic flat-faced shape before the design lift coefficient was exceeded.

To determine the thickness requirement, a combination of rule-of-thumb and simple bending strength calculations was used. The rule-of-thumb was that the section thickness to chord ratio should not be less than 7 percent at the 70 percent chordwise station, and that the nose thickness should be at least equal to that of the BuShips parent foil. The nose of the parent foil appears to have undergone moderate vibration during its high-speed test,<sup>4</sup> while more heavily loaded at  $C_L = 0.24$  than the TAP-1 would be at  $C_L = 0.14$ .

The computer programs used automatically form a smooth hydrofoil upper surface, by reducing the clearance of the predicted upper free streamline by 20 percent over the forward 70 percent of the chord, and by shifting it aft by 0.05 chordlength. The small region at the leading edge is fitted in with a wedge. From the 70 percent chord position to the trailing edge, a parabola is used, which matches the slope at the 70 percent chord station. From the section shape so formed, which is sharp at both the leading and the trailing edges, a series of 13 offsets are picked up, which are used to compute the section moment of inertia and the section area.

Then two possible locations for the neutral axis are assumed: one, a horizontal line through the centroid of the area, while the section is at its design angle of attack; the other, the midline or camberline of the section. From these lines fiber distances are computed to points on the surface of the section. The bending moment at the blade root is computed from the area of the blade and the loading on it, taking that loading corresponding to the section lift coefficient to be distributed uniformly all over the face of the blade. Then a maximum spanwise bending stress is computed from the formula

$$S_b = \frac{M C_t}{I_{xx}}$$

where  $M$  is the bending moment,  $S_b$  is spanwise bending stress,  $C_t$  is the distance from the assumed neutral axis to the furthest bending

fiber, and  $I_{xx}$  is the section moment of inertia (about its centroid). This stress is linearly distributed in the vertical direction.

The chordwise stress is computed by assuming that each spanwise section of the wing acts independently of the others in chordwise deformation. Essentially the nose of each section is assumed to be cantilevered about various chordwise stations, and the moment about each of these chordwise stations is computed from the distribution of loads forward of it. The minimum thickness of the section is computed at that station, and when this is combined with the computed moment in the linear formula for a solid cantilever beam stress, a value of stress at each of the chordwise stations may be found. The maximum value of this distribution is called Barr's chordwise nose stress.

#### THE DESIGN OF TAP-1 AND TAP-2

In the design of the two hydrofoils in question, both the chordwise and spanwise stresses were kept below 20 ksi maximum when the hydrofoil was operating at its design condition. However, the maximum stress in the model will occur at the off-design condition of maximum loading. If we assume that double lift is possible for lift control, then  $C_L \approx 0.30$ . However, the cavity could wash off the foil during a plunge into a wave, which would raise this value to  $C_L \sim 0.45$  (assumed). In that case, the model stress would be approximately 45 ksi, still within the yield limit of the material, 17-4 PH stainless steel heat-treated to 150 ksi for 2 percent yield.

It is obvious that several improvements to foil design can be made in the area of strength analysis. First, the maximum lift loading to be expected on the foil is not well known. Especially during wave broaching it is expected that the lift force could become very large, although it is doubtful that the lift coefficient could exceed the value  $C_L = 0.88$  which would occur for a foil plunging vertically into the water at speed. If the lift ever did get that high, the stress in the models would be very close to yield.

Another problem is fatigue stress in the thin leading edge. When other section parameters such as section modulus and lift coefficient are kept constant, then the section lift-to-drag ratio improves as the nose is made thinner. However, during testing these thin noses tend to vibrate at a frequency on the order of 3000 cps. Because the amplitude of this vibration has never been measured for a supercavitating hydrofoil, there is no way to know whether or when fatigue stress will be a problem, although leading edge failures have been observed during high speed testing.<sup>5</sup>

Furthermore, the stress analysis method as described above is faulty for several reasons:

1. It does not consider the chordwise variation in the loading.
2. Typical supercavitating sections experience their maximum loading at the thin leading edge, while linear beam theory predicts maximum stress at the thick trailing edge. Experiments have shown that linear beam theory is not adequate for triangular sections, and that the maximum stress occurs at about 50 percent chord.<sup>6,7</sup>
3. In the linear beam theory the location of the neutral axis must be assumed. While this apparently works well for thin airfoil sections, it does not apply to sections with wedge shape or with an annex.
4. Linear beam theory does not consider the interactions between the chordwise and spanwise stresses.

A direction for improvement would be to use either plate and shell theory or solid element theory, both of which have been incorporated into the Nastran system for example. The plate theory considers the load, thickness, and stress distributions to be piecewise constant, while the solid element theory can account for quadratic thickness variation and a piecewise linear variation in stress. However, both these systems as yet require more data preparation and

computer running time than the average designer can afford to invest in a single trial design. A running time of 200 to 400 seconds on the CDC 6400 might be an example for a single blade, which at current rates would equal about two hours of labor time.

While the system as described for fitting a parabolic top to the foil might suffice for a supercavitating foil, where the cavity length would be expected to be a problem, its use for a ventilated foil such as TAP-1 would waste much of the space in the cavity. For that reason the foil section for TAP-1 has a 30 percent annex. This is not as large as that of the Boeing annex foil.<sup>8</sup> The annex adds to the wetted lifting area during takeoff as well as adding structural strength. However, too large an annex can interfere with the cavity walls at off design angles of attack.

The section finally selected for the TAP-1 foil results from the parameter selection  $\beta = 0.08$ ,  $A_1 = 0.01$ ,  $A_2 = 0.0075$  in the Levi-Civita method. This means that the basic flat plate has an incidence angle of 0.08 radians, or  $4.58^\circ$ , against which the camber terms are superposed. Calculated two-dimensional properties are:

|          |                           |   |
|----------|---------------------------|---|
| $\alpha$ | = 4.616°                  | Chord inclination angle                                       |
| $C_L$    | = 0.136                   | Lift coefficient  |
| $L/D$    | = 12.95                   | Lift-to-drag ratio  |
| $\sigma$ | = 0                       | Cavitation number   |
| $C_M$    | = 0.049                   | Moment coefficient (LE)                                       |
| $I_{xx}$ | = $0.241 \times 10^{-4}$  | Section moment } Using the parabolic<br>Section modulus } top |
| $Z$      | = $3.6977 \times 10^{-4}$ |   |
| $S_n$    | = 12.4                    | Nose stress, normalized on $(1/2)\rho U^2$                    |

As stated, the top of this foil section was subsequently hand modified from the machine fitted parabola to add an annex to the rear. Also, the maximum thickness was slightly reduced and shifted forward, so that the top of the foil section lay just slightly beneath the free streamline as predicted for a cavitation number of  $\sigma = 0.05$  by using the parallel plate wake model from the Wu's 1955 method computer program. Then the nose thickness was checked to make sure that it was indeed equal to that of the parent foil.

The second foil section, TAP-2, was designed for cavitation number  $\sigma = 0.135$  by using Larock and Street's computer program, which uses Tulin's single spiral vortex wake model to represent the finite cavity length associated with flow at non-zero cavitation number, infinite stream. This program allows the designer to specify three different camber rates along the face of the section from leading edge to trailing edge. As typically used, and as in this case, the first camber rate is a very tight arc used to specify a blunt leading edge; the second controls the curvature in the nose region from 0 to 20 percent of chord; and the third camber rate controls the curvature of the remainder of the pressure face, and is essentially used to control the foil lift coefficient.

For the first foil, TAP-1, the section was chosen first to be a two-term of the correct lift and nose thickness and then the aspect ratio was calculated to have the main bending stress come out to be 45 ksi maximum and less than 20 ksi design. This resulted in a computed aspect ratio of 2.4, which was desirable both because TAP-1 was a ventilated foil and low aspect ratio was desirable to help the ventilated air distribution, and because studies of foils without struts had shown that L/D versus main bending stress improves with decreasing aspect ratio.<sup>2,9</sup>

For the TAP-2 supercavitating foil, for which air distribution would not be a problem, it was decided to use a larger aspect ratio,  $AR = 3$ . Knowing this plus the required lift coefficient, it was possible to calculate the main bending moment at the blade root, and hence the required section modulus to give a design stress less than 20 ksi.

For the supercavitating TAP-2 it was decided to do without the annex and in fact to use a hand-faired top with a sharp trailing edge. This is because the natural cavity was expected to be quite short for the following reasons:

1. Low lift coefficient
2. Near surface effect
3. Three-dimensional effect

and because of published photographs<sup>4</sup> showing short natural cavities under certain conditions near the 80 knot speed for which this foil was to be designed. With these constraints in mind a final section shape was selected by hand-varying the parameters in the program, trying to make the nose region as thin as possible consistent with structural integrity and the experience with the parent foil. A recurring problem during design was low section L/D caused by trying to get a low  $C_L \sim 0.14$  at a cavitation number  $\sigma = 0.135$ . In order to have enough thickness with this combination of parameters, the camber of the main body generally had to be made negative. An increase in the thickness of the nose, while increasing the L/D, would add more lift in that region, which would have to be compensated for by more negative camber in the body if the body thickness were to be maintained. This process came to a halt when the body face pressure coefficient reached zero, but before the blunt nose was as thin as would be consistent with an L/D in the 12-13 range.

When the section shapes became available for both of the hydrofoils (see Figure 1), it was necessary to lay out the three-dimensional form of the models. An area for each of 75 square inches had been selected to match that of the original parent foil. Besides wishing to have the parent foil data as part of the series, it was also desirable to have this large size of model to minimize the effect of machining imperfections, and because there is apparently an effect of Froude number on model flutter speed which favors low Froude number models (large size).

The taper ratio for model TAP-1 had previously been chosen to be tip chord/root chord =  $\tau$  = 0.5, based on theoretical work of Nishiyama<sup>10</sup> showing an optimum for  $0.3 \leq \tau \leq 0.5$ , and on previous experimental work.<sup>5,11</sup> For the Model TAP-2, which without an annex required a more painstaking structural design, a taper ratio of 0.33 was selected, to more evenly distribute the bending stress along the span and to reduce the stress calculated at the blade root using simple beam theory.

The remaining planform parameter, sweepback, was more difficult to select. Experiments have shown that increasing blade sweepback degrades the hydrodynamic properties of a wing.<sup>5</sup> However, in compensation, sweepback has been shown to increase the wing's flutter speed,<sup>12</sup> and leading edge sweepback is known to reduce the stresses in the thin leading edge.<sup>13</sup> However, too much blade sweepback, such as in a highly skewed propeller, can lead to stress concentrations at the root near the chordwise trailing edge, caused by having the center of loads aft of the trailing edge, where it generates a torque on the blade.

Because the reasonably large taper of the two models meant that the leading edge was already swept back appreciably, it was decided that the overall blade sweep did not need to be very large, and that in any case the center of blade loads should not move past the trailing edge since a reliable stress analysis method is not available, and it was not possible to calculate in advance how much benefit the sweepback would produce to the flutter speed. Since having the 50 percent chordline of the spanwise sections perpendicular to the center line would be the definition of zero-sweep of the midchord line, it was decided that making



the 70 percent chordline perpendicular to the centerline would be a reasonable amount of sweepback without invalidating the stress analysis. Furthermore, since supercavitating hydrofoils typically use a 30 percent chord flap,<sup>1</sup> this would allow for a straight hingeline if flaps were to be added to some later model.

After the planform and section shape had been selected as shown in Figure 2, the next problem was to select a spanwise twist of the sections in such a manner that the cavity wall above the sections would be smooth above the foil at the design angle of attack. Until a realistic stress analysis method became available, there seemed to be no reason for changing the thickness of the sections in the spanwise direction, since linear beam theory predicted a smooth bending stress variation spanwise for tapered wings, and since experiments had shown that the chordwise stresses became appreciable near the wing tips as the spanwise stress diminished.<sup>6</sup> Therefore, the wing sections were made geometrically similar along the span.

The defining line for the sections was the wetted trailing edge, which line when followed spanwise remained always in the plane of the angle of attack (a plane inclined at the foil angle of attack to a horizontal plane) in such a way that the hydrofoil model as a whole had very little dihedral angle, although this particular line was then raised somewhat (see Figure 3). The use of dihedral to prevent broaching is not necessary on a ventilated foil model, while calculations were not available as to how much dihedral might be necessary to generate side forces.

All the wing sections were twisted about the wetted trailing edge. Three types of spanwise twists were superposed:

- a. Three-dimensional downwash correction due to trailing vortex sheet.

- b. Strut downwash due to strut thickness.
- c. Upwash due to free surface proximity.

The three-dimensional downwash angles were taken from Altmann's foil design report,<sup>14</sup> based on the lift coefficient, aspect ratio, taper ratio, and sweep angle of our wings. Unfortunately his curves, called Katzoff's corrections, are only for a vortex sheet, and do not include the effect of the cavity thickness.

The strut downwash angles were taken from experimental data reported by Altmann and Elata<sup>15</sup> for ventilated hydrofoils, using a 12 percent parabolic strut. Their values were multiplied by 1-1/2 for the TAP-1 foil which used an 18 percent parabolic strut, and were left unchanged for the TAP-2 and its 12 percent parabolic strut. That curve for the downwash angle of midchord ( $X/C = 50\%$ ) was used. Note that the curves only extend spanwise for a distance of one strut chord. The free surface upwash angle of  $1.48^\circ$  was calculated for a flat plate at  $d/c = 1$  and the design  $C_L$ , and then applied linearly over the span as the depth/chord ratio varied spanwise, according to a linear formula from Altmann's report,<sup>14</sup>

$$\Delta\alpha = K \frac{C_L c}{b}$$

The three spanwise twist angle components were then added algebraically to give a total spanwise twist correction, shown in Figure 4. The resulting "J" shaped curve was a maximum near the strut, declined to negative near the blade midspan and then increased again near the blade tip vortex. Qualitatively, the curve much resembles the "J" shaped curve of the length of short leading edge cavities shown in photographs of foils at low angle of attack,<sup>4</sup> where the cavity tends to wash off first near the strut and near the wing tips.

The choice of strut for a supercavitating hydrofoil is always difficult. In this particular case, a parabolic section was chosen for its positive pressure characteristics at high speeds. Both foils TAP-1 and TAP-2 have the same planform area as the BuShips parent foil. However, the parent foil with its 5-inch 15 percent thick strut failed to ventilate repeatedly during its high-speed test.<sup>4</sup> Therefore, it was decided to enlarge the strut size in relation to the foil area for the ventilated TAP-1 model, to a 6-inch strut at 18% thick. For the second foil, TAP-2, ventilation was not necessary so a 12 percent thick strut was used, the 12 percent figure being a rule of thumb for a minimum strut thickness, and the 6-inch chord figure chosen so that the strut could be compared to the first model. The two struts thus could be interchanged between the two foils, in such a way that the vent air supply to the foils could be changed by changing the thickness of the base-vented strut. Both struts are solid although the 18 percent strut has provision for an encased air passage to be attached to its base to prevent ventilating air from being entrained into the strut wake. A strut sweepback angle of 12° was chosen for both foils, so that even at the maximum foil angle of attack of 15° (i.e., 10° above design angle) there would still be a slight sweepback angle. A strut vertical length of 30 inches was chosen to provide maximum 3-foil depths immersion plus a foot of clearance for the dynamometer over the water.

Besides being designed to allow strut interchangeability, the foil-strut mounting area provides for a stub to be cut to the strut contour. This stub, about 3/4" high, is an integral part of the original 2" thick plate from which the foil would be machined. The stub is also filleted at its base, and sharpens along its leading edge to prevent downwash generation. In this way it is hoped that the usual stress concentration in the strut mounting area, which usually leads to cracks around the screwholes, can be avoided. A thin tip plate is also allowed for the TAP-2 foil, again part of the original plate, since there is no problem of interfering with tip vortex ventilation for a supercavitating hydrofoil model.

The choice of 17-4 PH stainless steel as the foil material was made for several reasons. First, it is non-corroding (unless pitted or cracked); second, it is preferred by shop technicians because it holds its shape when worked on or heated; and third, it can be heat-treated to a variety of hardness numbers and combinations of ultimate and fatigue stress. Finally, like all steels, it has a high value of Young's modulus, which limits the magnitude of deflections and vibrations, to which supercavitating hydrofoil models, in their quest for thin sections and low drag, will always be sensitive.

#### PLANNING FOR A TEST PROGRAM

Any decision to resort to expensive, physical testing of high-speed hydrofoil concepts is motivated by the desire for answers to questions not readily approached theoretically. In this regard, the natural problem areas are:

1. Takeoff performance - prediction of which is problematical because only linearized theory is available for the three-dimensional hydrofoil case, which theory is not valid at the large incidence angles associated with takeoff. (See Reference 1.)
2. Ventilation characteristics - cannot be predicted theoretically, either the amount of air flowing down the strut, or how much is entrained in the foil cavity. For a recent empirical treatment of this subject, see Reference 16.
3. Deformation and vibration - as explained in the text, the state of theoretical prediction is very poor for stresses in wedge-shaped hydrofoil sections. Furthermore, the hydrodynamic pressure varies with the wing deflection in such a way that many of the natural modes of vibration are distorted. Also, there is a periodic driving force on supercavitating foils due to vortex shedding.

Therefore, to establish a model's validity in steady flow, two tests would be planned, one at the takeoff speed (60 fps), and one at the cruise speed (135 fps).

The takeoff test would concentrate primarily on finding the most favorable combination of flap angle and angle of incidence for takeoff at various depths. Also it would be desirable to measure the cavity length in order to avoid those combinations of parameters for which short cavities occur and vortex shedding is a problem. It would be expected that both the strut and the foil would have vapor cavities longer than one chord during this test. A maximum flap deflection angle of  $30^\circ$  might reasonably be expected to be employed.

The cruise speed test would be concerned with those phenomena which could not adequately be measured or represented in a simulated speed facility. Among the quantities to be measured would be the variation of forces over a range of angle of attack and depth, and the pressure in the foil cavities. Also for the TAP-1 model which was designed to run in the fully ventilated condition, it would be desirable to measure the operational boundaries within which the ventilated flow regime could be maintained, in a field of depth-to-chord ratio and angle of attack. The ventilated regime might be initiated by dropping the foil vertically in the water at speed to the preselected depth, and the persistence of ventilation would be amenable to detection photographically. These boundaries of the ventilated flow regime in an  $\alpha - \sigma_v$  plane might be expected to depend partly on which of three possible strut combinations was used, i.e., 18 percent strut, 18 percent strut with enclosed air passage, or 12 percent strut. Finally, it would be observed whether the leading edge sweepback alleviates the edge vibration observed on the parent foil. Also concerned with vibrations, it would be hoped that the amplifiers for the force measuring system could pick up the less than 5000 cps signals which might result if there were natural cavity vortex shedding which had an effect on the foil forces.

## POSSIBLE IMPROVEMENTS TO THE DESIGN METHOD

Of the possible alternatives in foil design, that of simulating the performance of the entire wing system by building it up out of individual linearized elements, such as source sheets for thickness, source rods for axial pods, and vortex sheets for lift elements, is perhaps not as desirable as it would initially appear. The method has been available for subsonic aircraft design for some time, and also has been extended to subcavitating hydrofoils.<sup>17</sup> Perhaps what the method lacks most is precision, for the number of matrix elements necessary to account exactly for all the possible elemental interactions is usually larger than the program user can tolerate. Therefore, this method has difficulty explaining the detailed behaviour of one single part of a complex structure. While some notable strides toward writing such a program have been taken, its final development appears to be many years in the future.<sup>18,19,20</sup>

In the meantime, foil designs could be improved by developments in several areas. One of the most critical at present is the prediction of structural properties. Since supercavitating hydrofoil lift-to-drag ratio is very sensitive to both body and leading edge thickness, the development of a reliable stress analysis method could improve foil performance quite considerably just by making available for use all the stress in the material. But any proposed method would probably have to use less than 300 seconds on the CDC to be worthwhile.

The development of vibrations criteria is a bit more complicated, but the unsteady force data which would be obtained from a high-speed test of one of the hydrofoils would help to determine what should be the relation between fatigue stress and ultimate stress, and thus help in the selection of the alloy for a supercavitating hydrofoil model. Force data in waves would also be useful for this purpose.

The leading edge vibration problem will probably remain intractable until the amplitude of the vibration can be determined, from which can

be determined the unsteady leading edge stress. One way to do this might be to mount a Doppler velocimeter above the foil leading edge, to measure the leading edge deflection rate. Or an accelerometer or strain gauge could be embedded in the foil material.

Better methods of determining the spanwise twist rate will probably be developed in the next several years as lifting surface programs are perfected for supercavitating hydrofoils. However, there is still a need for experimental measurements of three-dimensional cavity surface locations above ventilated and supercavitating hydrofoils, data with which to check the theoretical predictions.

Another problem not yet well resolved is to determine how big the strut size should be to ventilate a given foil area. A possible high speed test of a foil with several strut sizes would help to answer this problem, which was also addressed by Ejata, who found that foils with larger struts could indeed remain ventilated deeper. A question arises as to whether a ventilated foil with a large strut, and a higher foil L/D but a larger strut drag, would have a higher system L/D than a supercavitating model which could use the minimum possible strut thickness.

This is related to the problem of how to scale the ventilated boundaries up to prototype craft size. So far as is known, there have been no measurements of ventilation boundaries for geosimilar, blunt-based strut supercavitating foil combinations. The flow of compressible fluid such as air may be non-linear in the size parameters, and therefore linear size scaling or Froude Law scaling may not apply.

In summary, possible improvements in the design procedure would be:

- a. adequate stress analysis

- b. accurate three-dimensional downwash prediction
- c. three-dimensional cavity location measurements
- d. strut size versus foil size relation

#### DESIGN OF VENTILATION DOORS

As is well known, the air supply required to maintain a ventilated condition of a hydrofoil increases quite drastically with speed, (see for example Reference 23) and the mere presence of a parabolic strut above the foil is generally not enough to insure a cavitation number in the ventilated range (say  $\sigma < 0.03$ ) at high actual water speeds. For example, the high-speed tests of Virgil Johnson failed to fully ventilate an aspect ratio three hydrofoil at depth/chord 0.8 (Reference 24), or a base ventilated hydrofoil (Reference 25) even though both had parabolic struts. The high-speed test of the BuShips parent hydrofoil (Reference 4) also showed a failure to ventilate below depth/chord one-half above a certain speed (approximately 60 knots). This problem was addressed by Wadlin (Reference 26) near the end of the NASA high-speed hydrofoil program, who solved it by adding vent wings to the side of the strut to enlarge the strut cavity. The cavitation number could not be brought to zero by this method but could be reduced to the range  $0.01 < \sigma < 0.03$ , which would correspond to a ventilated flow.

Subsequently vent wings were included in the design of the Boeing annex foil. Although they doubled the strut drag, most of the cavity pressure measurements reported at high speed (80 knots) included their use (Reference 27). The design used appears from the report to be effective down to depth/chord 2.2

For the ventilated TAP-1 foil, it was intended that the foil be tested both with an 18% and an 12% thick strut, which presumably would provide two different air ventilation rates. Since the vent wings provide no structural strength while doubling the strut drag,



it was hoped that the 18% thick strut could ventilate the foil through its own thickness, thereby providing more structural strength and transmission space while supporting the larger cavity. Consequently, the vent wings designed for the 18% thick strut, using a 15° wedge angle, are merely surface spray deflectors to protect the cavity opening. But the strips selected for the 12% thick strut, using a 30° wedge angle, are similar in relative size to those on the annex foil, and were designed to enlarge the strut cavity considerably. These wing doors were designed to flare out slightly near the strut-foil intersection when the 12% thick strut was used, since the TAP-1 foil was to be built with an 18% thick integral mounting stub. The 3/8" wedge chord for both spray deflectors was relatively the same as that used with the annex foil. The approximate layout of the spray deflectors is shown on Figure 5. Unquestionably the use of straight untapered wedges is not optimum from a drag point of view, however, functional they are expected to be. It is expected that design changes would be suggested by photographs of the high speed flow, and indeed that the mounting and submergence of these spray wedges might be adjusted during any possible testing.

It might be noted here that since the initial acceleration of the testing carriage to be used at Langley Field, Virginia is approximately 3 to 4 g, there should not be any problem in establishing an initially ventilated cavity, since the water can only fill in the cavity with a maximum acceleration of 1 g (Reference 28). This is in distinction to ordinary towing basin practice, where with an initial towing carriage acceleration of 0.5 g, supercavitating hydrofoils consistently refuse to ventilate at depth/chord one unless special techniques are used to trigger the initially ventilated condition (Reference 29). This might explain for instance the discrepancy in data between Spangler's report of high-speed towing tests of the BuShips parent foil (Reference 4) and the indoor towing test of the exact same foil (Reference 30) where for identical towing speeds, depth of submersion and angle of attack, the foil ventilated to depth/chord

1-1/2 during the outdoor test and to depth/chord 1/2 during the indoor test

### FOIL PERFORMANCE PREDICTION - TAP-1

Foil Drag: At cruise (80 knots) condition

Foil weighted average twist angle of  $\sim 1.5^\circ$  will reduce the L/D to  $\sim 10.5$  geometrically.

Design Load = 1300 lb<sub>f</sub>

Foil Drag  $\sim 124$  lb<sub>f</sub>

Strut drag: based on data from the Aerojet-General Report (Reference 31), a strut drag coefficient (based on strut chordlength and depth) of .013 for the 18% strut and 0.009 for the 12% strut might be expected

18% strut: drag =  $.013 \times 127\text{psi} \times 6'' \times 6'' = 60$  lb<sub>f</sub>

12% strut: drag =  $.009 \times 127\text{psi} \times 6'' \times 6'' = 40$  lb<sub>f</sub>

However, the large size spray wedges used with the 12% strut will probably double its drag, (according to the report on the annex foil) while the smaller spray wedges used with the 18% thick strut might increase its drag only half again. So we assume

|           |                         |
|-----------|-------------------------|
| 18% strut | 90 lb <sub>f</sub> drag |
| 12% strut | 80 lb <sub>f</sub> drag |

Then the foil system L/D's, which will presumably be unchanged whether the foil ventilates or not, will be

|           | L/D | L/D with Wedges |
|-----------|-----|-----------------|
| 18% strut | 7.0 | 6.1             |
| 12% strut | 7.9 | 6.4             |

at the cruise speed of 80 knots or 135 fps

TAKEOFF PERFORMANCE:

We assume a vapor cavitation number  $\sigma_v = 0.6$ , at 35 knots (60 fps), and takeoff at depth/chord = 3, with a combination of flap and angle of attack. The struts are assumed to be partially ventilated to  $\sigma = 0.3$  while the foil is assumed to be operating in the supercavitating mode with a cavity length greater than one chord. Strut drag coefficients are assumed to be  $C_D = 0.017$  for the 18% thick strut, and  $C_D = 0.012$  for the 12% thick strut. Then the strut drag is

$$18\% \text{ strut: } 0.017 \times 25 \text{psi} \times 6'' \times 18'' = 46 \text{ lb}_f$$

$$12\% \text{ strut: } .012 \times 25 \text{psi} \times 6'' \times 18'' = 32 \text{ lb}_f$$

On the foil model, the extra area of the annex means that the required lift coefficient will be

$$C_{L_{\text{req'd}}} = 5.22 \times 0.14 \times 1/1.33 = 0.56$$

The strut downwash will be assumed twice that of design due to the increased depth, or an average value of  $2^\circ$ . The three dimensional effect for this planform is again taken from Altmann's curves (Reference 14) where

$$K_i = 10 = \alpha_i / C_L, \text{ or } \alpha_i = 6^\circ$$

so total downwash  $\sim 8^\circ$ , which will decrease  $C_L$  by  $\pi/2 \times 8^\circ \times \pi/180$  or 0.22. Hence a section lift coefficient of  $C_L \sim 0.77$  will be required for takeoff. When we compare the section characteristic calculations of Wu and Wang (Reference 32), we see that at  $\sigma = 0.6$  this lift coefficient is readily attainable with a flat plate of

body angle  $10^\circ$  and flap deflection  $10^\circ$ . Then the section L/D is 3.9. Thus for a  $1300 \text{ lb}_f$  foil load at takeoff, the foil drag would be  $330 \text{ lb}_f$ . Thus at takeoff

|           |           |
|-----------|-----------|
| 18% strut | L/D = 3.5 |
| 12% strut | L/D = 3.6 |

However, a caveat should be made here that experimental results for flapped supercavitating hydrofoils at takeoff conditions rarely show a lift to drag ratio much in excess of 3.0, see for example Conolly (Reference 1).

#### REFERENCES

1. Conolly, A. C., "Experimental Investigations of Supercavitating Hydrofoils with Flaps," Main Volume plus Appendix A, General Dynamics/Convair GD/C-63-210, Dec 1963
2. Kermeen, R. W., "Experimental Investigations of Three-Dimensional Effects on Cavitation Hydrofoils," Journal of Ship Research, Sep 1961
3. Auslaender, J., "Low Drag Supercavitating Hydrofoil Sections," Hydronautics, Inc., TR 001-7, Apr 1962
4. Spangler, P. K., "Performance and Correlation Studies of the BuShips Parent Hydrofoil at Speeds from 40 to 75 Knots," NSRDC Report 2353, Dec 1966
5. Wright, H. R., Jr., "Experimental Study of High Speed Hydrofoils," Volumes I and II, Grumman Aircraft Engineering Corporation, Report XAR-A-45, Aug 1963
6. McCarthy, J. H. and Brock, J. S., "Static Stresses on Wide-Bladed Propellers," Journal of Ship Research, Jun 1970
7. Morita, S., "Model Propeller Blade Structure Test to Determine Optimum Sweepback Angle," and "Full Scale Supercavitating Propeller Blade Structure Test," DeHavilland Aircraft of Canada Ltd., Report HF 1-S-G-3/1 and 2, 1966
8. Jones, F. D., "Final Summary Report - Annex Foil Development Program," Boeing Co., Aero-Space Div., Report D2-20348-1, Jan 1964

9. Miller, E., Jr., Altmann, R., Poquette, G., and Lain, H., "A Parametric Analysis of Fast Hydrofoil Configurations," Hydronautics Inc., TR 7224-1, Nov 1972
10. Nishiyama, T., "Lifting-Line Theory of Supercavitating Hydrofoil of Finite Span," ZAMM, 50, 643-653, 1970
11. Dobay, G. F., "Influence of Scale Ratio, Aspect Ratio, and Planform on the Performance of Supercavitating Hydrofoils," NSRDC Report 2390, Aug 1967
12. Squires, C. E., Jr., "Hydrofoil Flutter, Small Sweep Angle Investigation - Final Report," Grumman Aircraft Engineering Corp., Report DA Nonr-3989.3, Nov 1963
13. Davis, B. V. and English, J. W., "The Evolution of a Fully Cavitating Propeller for a High-Speed Hydrofoil Ship," Office of Naval Research Hydromechanics Symposium, 1968
14. Altmann, R., "The Design of Supercavitating Hydrofoil Wings," Hydronautics, Inc., TR 001-14, Apr 1968
15. Altmann, R., and Elata, C., "Effects of Ambient Conditions, the Gravity Field, and Struts on Flows over Ventilated Hydrofoils," Hydronautics, Inc. TR 605-1, May 1967
16. Elata, C., "Choking of Strut-Ventilated Foil Cavities," Hydronautics, Inc. TR 605-2, May 1967
17. Richardson, J. R., "Pressure Distribution on a Hydrofoil of Finite Span Near the Free Surface," Engineering Research Associates - Canada, Report ERA-C 53/3, Jun 1966
18. Widnall, S. E., "Unsteady Loads on Supercavitating Hydrofoils of Finite Span," Journal of Ship Research, Vol. 10, No. 2, Jun 1966 pp. 107-118
19. Tsen, L. F. and Guilbaud, M., "Methode due Potentiel d'Acceleration Pour Le Calcul des Ailes Supercavtantes Finies," Bulletin de L'Association Technique Maritime et Aeronautique (ATMA) No. 70 1970
20. Nishiyama, T., "Linearized Theory of a Supercavitating Hydrofoil by Singularity Method - Second Report - Three Dimensional Flow," Technology Reports, Tohoku University, Vol. 33 No. 2, 1968
21. Wu, T. Y., "A Free Streamline Theory for Two-Dimensional Fully-Cavitated Hydrofoils," Journal Math. Phys. Vol. 35, No. 3, 1956 pp. 236-265

22. Larock, B. E. and Street, R. L., "Cambered Bodies in Cavitating Flow- A Nonlinear Analysis and Design Procedure," Journal of Ship Research Vol. 12, No. 1, Mar 1968
23. Schiebe, F. R. and Wetzel, J. M., "Ventilated Cavities on Submerged Three-Dimensional Hydrofoils," University of Minnesota, St. Anthony Falls Hydraulic Laboratory, Technical Paper No. 36, Series B, Dec 1961
24. Christopher, K. W. and Johnson, V. E., Jr., "Experimental Investigation of Two Low-Drag Supercavitating Hydrofoils at Speeds up to 200 Feet per Second," NASA TN D-436, Aug 1960
25. Johnson, V. E., Jr. and Rasnick, T. A., "Investigation of a High-Speed Hydrofoil with Parabolic Thickness Distribution," NASA TN D-119, Nov 1959
26. Wadlin, K. L., "Ventilated Flows with Hydrofoils," Presented at the Twelfth General Meeting of American Towing Tank Conference, University of California, Aug 1959
27. Gornstein, R. J. and Holgate, T. A., "Depth Effects on Hydrodynamic Characteristics of the Annex Foil at 80 Knots," Boeing Company Report Number D2-82505-1, Feb 1965
28. Personal communication with Mr. Douglas L. Gregory, Naval Ship Research and Development Center, Bethesda, Maryland 20034.
29. McGehee, J. R. and Johnson, V. E., Jr., "Hydrodynamic Characteristics of Two Low-Drag Supercavitating Hydrofoils," NASA Memo 5-9-59L, Jun 1959
30. Dobay, G. F., "Performance Characteristics of the BuShips Parent Foil," NSRDC Report 2084, Aug 1965
31. Levy, J., "Hydrodynamic Characteristics of Base-Vented and Supercavitating Struts for Hydrofoil Ships," Aerojet General Corporation, VonKarman Center, Oceanics Products Division, Report No. 2796, Aug 1964
32. Wu, T. Y. and Wang, D. P., "A Wake Model for Free-Streamline Flow Theory, Part II: Cavity Flows Past Obstacles of Arbitrary Profile," Hydrodynamics Laboratory, C.I.T., Report No. 97-4, May 1963

TABLE 1  
COMPARISON OF NUMERICAL CHARACTERISTICS

|                                     | BuShips Parent                               | TAP-1   | TAP-2   |
|-------------------------------------|--|---|---|
| <u>Planform</u>                     |  |   |   |
| Area                                | 75 sq. inches                                | 75 sq. inches   | 75 sq. inches   |
| Aspect Ratio                        | 3  | 2.4   | 3   |
| Centerline Chordlength              | 5 inches                                     | 7.5 inches  | 7.5 inches  |
| Tip Chord                           | 5 inches                                     | 3.75 inches   | 2.5 inches  |
| Taper Ratio                         | 1  | 0.5   | 0.33  |
| Un swept Chordline                  | 50%  | 70%   | 70%   |
| Sweepback at Midchord               | 0°   | 6.42°   | 7.58°   |
| Spar                                | 15 inches                                    | 13.33 inches  | 15 inches   |
| Annex Percentage of Wetted Chord    | 0  | 33%   | 0   |
| <u>Strut Size</u>                   |  |   |   |
| Section                             | Parabolic                                    | Parabolic   | Parabolic   |
| Chord                               | 5 inches                                     | 6 inches  | 6 inches  |
| Thickness                           | 15%  | 18%   | 12%   |
| Sweepback                           | 0°   | 12°   | 12°   |
| <u>Foil Section Characteristics</u> |  |   |   |
| Definition                          | Tulin Two-Term                               | Levi-Civita Two-Term  | Larock and Street three parameter   |
| Program and Inputs                  | linearized two-dimensional with free surface | Wu's 1955 program non-linear two-dimensional (parallel plate wake model) in infinite stream | non-linear two-dimensional using Tulin single spiral vortex wake model in infinite stream |
|                                     | $d/c = 1, X=0.0875, c=2.5, \tau=0$           | $\beta=.08, A_1=.01, A_2=.0075, \epsilon=0$   | $K=1.12, t_b=.04, t_1=-.04, t_2=-.16, A_1=.09, A_2=.03, A_3=.012$                         |

|  | BuShips Parent            | TAP-1   | TAP-2                     |
|--|---------------------------|---|---------------------------|
| Design Cavitation No.                      | 0                         | 0 - 0.05  | 0.135                     |
| Lift Coefficient                           | 0.17                      | 0.1366  | 0.1396                    |
| Ratio of Lift to Drag                      |                           | 12.95   | 10.64                     |
| Pitching Moment Coefficient (leading edge) |                           | 0.049   | 0.052                     |
| Center of Pressure from leading edge       |                           | 36%   | 37%                       |
| Thickness to Chord Ratio (maximum)         | 13.1%                     | 8.6%  | 6.3%                      |
| <u>Structural*</u>                         |                           |   |                           |
| Area/Unit Chord                            | 0.0599                    | 0.0530  | 0.0478                    |
| Section moment/unit chord                  | $0.423 \times 10^{-4}$    | $0.265 \times 10^{-4}$  | $0.167 \times 10^{-4}$    |
| Section Modulus/unit chord                 |                           |   |                           |
| N.A. Horizontal Through Centroid           | $0.52 \times 10^{-3}$     | $0.41 \times 10^{-3}$   | $0.36 \times 10^{-3}$     |
| N.A. Midline                               | $0.65 \times 10^{-3}$     | $0.61 \times 10^{-3}$   | $0.53 \times 10^{-3}$     |
| Actual Section Modulus at Centerline       |                           |   |                           |
| N.A. Horizontal                            | 0.065 inches <sup>3</sup> | 0.173 inches <sup>3</sup>   | 0.152 inches <sup>3</sup> |
| N.A. Midline                               | 0.081 inches <sup>3</sup> | 0.257 inches <sup>3</sup>   | 0.224 inches <sup>3</sup> |
| Leading Edge Radius                        | 0.002 inches              | (Lapped)  | 0.02 inches               |
| Leading Edge Stress at Design              |                           | $12.4 \times 1/2AU^2$   |                           |
| Material                                   | Stainless Steel           | 17-4 PH<br>Stainless Steel<br>heat treatment H1075<br>Rockwell Hardness C36 | 17-4 PH Stainless         |

\*NOTE - Section data for TAP-1 does not include annex.



|  | BuShips*                     | TAP-1                      | TAP-2                        |
|--|------------------------------|----------------------------|------------------------------|
| <u>Simple Bending Stress Calculation</u><br>(Assumes constant section lift)              |                              |                            |                              |
| Equivalent Force =<br>80 knot loading X<br>1/2 area = 128psi X<br>7 1/2 X C <sub>L</sub> | 818 lb <sub>f</sub>          | 655 lb <sub>f</sub>        | 672 lb <sub>f</sub>          |
| Blade Centroidal<br>Distance from Strut  | 3.75 inches                  | 2.96 inches                | 3.12 inches                  |
| Centerline Bending<br>Moment   | 3070 lb <sub>f</sub> -inches | 1940 lb <sub>f</sub> -inch | 2100 lb <sub>f</sub> -inches |
| <u>Design Stress</u>   |                              |                            |                              |
| <u>Calculated</u>  |                              |                            |                              |
| N.A. Horizontal  | 47 ksi                       | 11 ksi                     | 14 ksi                       |
| N.A. Midline   | 38 ksi                       | 8 ksi                      | 9 ksi                        |
| Design Load  | 1600 lb <sub>f</sub>         | 1300 lb <sub>f</sub>       | 1300 lb <sub>f</sub>         |

\*NOTE that lift corrections due to downwash are not included for the parent foil. These would reduce the lift and the stress significantly.

TABLE 2  
SECTION OFFSETS

| BuShips Parent Foil | TAP-1 |                |                | TAP-2          |                |                |
|---------------------|-------|----------------|----------------|----------------|----------------|----------------|
|                     | X     | Y <sub>L</sub> | Y <sub>U</sub> | X <sub>L</sub> | Y <sub>L</sub> | Y <sub>U</sub> |
| .025                | .005  | .0000          | .0017          | -.00077        | -.00054        | .0008          |
| .050                | .0125 | .0001          | .0034          | -.00130        | -.00115        | .0017          |
| .075                | .025  | .0002          | .0058          | -.00165        | -.00181        | .0032          |
| .100                | .05   | .0004          | .0098          | -.00181        | -.00250        | .0049          |
| .150                | .075  | .0006          | .0134          | -.00181        | -.00319        | .0071          |
| .200                | .10   | .0008          | .0169          | -.00142        | -.00431        | .0108          |
| .250                | .15   | .0013          | .0233          | -.00055        | -.00528        | .0127          |
| .300                | .20   | .0018          | .0294          | .00094         | -.00596        | .0141          |
| .400                | .25   | .0022          | .0352          | .0023          | -.0063         | .0150          |
| .500                | .30   | .0026          | .0408          | .0039          | -.0067         | .0150          |
| .600                | .35   | .0029          | .0462          | .0080          | -.0075         | .0150          |
| .700                | .40   | .0032          | .0515          | .0157          | -.0089         | .0150          |
| .800                | .45   | .0034          | .0564          | .0253          | -.0103         | .0150          |
| .900                | .50   | .0036          | .0609          | .0368          | -.0117         | .0150          |
| 1.000               | .55   | .0036          | .0651          | .0455          | -.0124         | .0150          |
|                     | .60   | .0036          | .0689          | .1055          | -.0171         | .0138          |
|                     | .65   | .0035          | .0725          | .1844          | -.0228         | .0120          |
|                     | .70   | .0032          | .0757          | .2773          | -.0291         | .0101          |
|                     | .75   | .0029          | .0786          | .3797          | -.0355         | .0087          |
|                     | .80   | .0025          | .0811          | .4872          | -.0417         | .0061          |
|                     | .85   | .0021          | .0833          | .5962          | -.0476         | .0039          |
|                     | .90   | .0015          | .0849          | .7037          | -.0528         | -.0005         |
|                     | .95   | .0008          | .0861          | .8075          | -.0573         | -.0145         |
|                     | 1.00  | .0000          | .0868          | .9060          | -.0612         | -.0378         |
|                     | 1.05  |                | .0872          | .9979          | -.0643         | -.0643         |
|                     | 1.10  |                | .0873          |                |                |                |
|                     | 1.15  |                | .0873          |                |                |                |
|                     | 1.20  |                | .0871          |                |                |                |
|                     | 1.25  |                | .0866          |                |                |                |
|                     | 1.30  |                | .0857          |                |                |                |
|                     | 1.33  |                | .0850          |                |                |                |

Rotate 3° for design angle

Rotate 4.62° for design angle

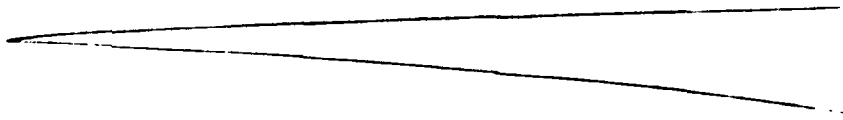
TABLE 3

TAP-1

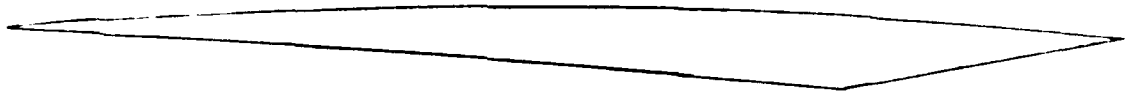
| Spanwise Position | Angle Correction, degrees |       |              | Total |       |
|-------------------|---------------------------|-------|--------------|-------|-------|
|                   | 3d                        | Strut | Free Surface |       |       |
| Basis for         | 0                         | 2.10  | 5.10         | -1.98 | 5.22  |
| TAP-1 Foil        | 0.025                     | 1.92  | 4.50         | -1.94 | 4.48  |
| Design with       | 0.05                      | 1.75  | 3.90         | -1.92 | 3.73  |
| 18% strut         | 0.075                     | 1.68  | 3.41         | -1.90 | 3.19  |
|                   | 0.10                      | 1.45  | 3.00         | -1.86 | 2.59  |
|                   | 0.15                      | 1.22  | 2.33         | -1.81 | 1.74  |
|                   | 0.20                      | 1.07  | 1.86         | -1.76 | 1.17  |
|                   | 0.25                      | 0.92  | 1.53         | -1.73 | 0.72  |
|                   | 0.30                      | 0.81  | 1.26         | -1.68 | 0.39  |
|                   | 0.35                      | 0.74  | 1.07         | -1.62 | 0.19  |
|                   | 0.40                      | 0.67  | 0.90         | -1.57 | 0.00  |
|                   | 0.45                      | 0.61  | 0.77         | -1.52 | -0.14 |
|                   | 0.50                      | 0.56  | 0.66         | -1.48 | -0.26 |
|                   | 0.55                      | 0.53  | 0.56         | -1.43 | -0.34 |
|                   | 0.60                      | 0.50  | 0.48         | -1.38 | -0.40 |
|                   | 0.65                      | 0.49  | 0.39         | -0.32 | -0.44 |
|                   | 0.70                      | 0.50  | 0.35         | -1.27 | -0.43 |
|                   | 0.75                      | 0.53  | 0.27         | -1.22 | -0.42 |
|                   | 0.80                      | 0.60  | 0.23         | -1.18 | -0.35 |
|                   | 0.85                      | 0.71  | 0.17         | -1.13 | -0.25 |
|                   | 0.90                      | 0.94  | 0.14         | -1.07 | +0.01 |
|                   | 0.925                     | 1.07  | 0.11         | -1.04 | +0.14 |
|                   | 0.95                      | 1.26  | 0.08         | -1.02 | +0.32 |
|                   | 0.975                     | 1.54  | 0.06         | -1.00 | +0.60 |
|                   | 1.000                     | 1.98  | 0.03         | -0.98 | +1.03 |

TABLE 4  
TAP-2

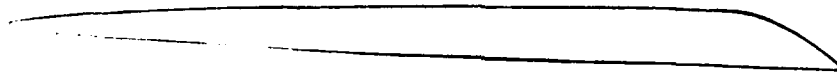
| Spanwise Position | Angle Correction, degrees |       |              |       |
|-------------------|---------------------------|-------|--------------|-------|
|                   | 3d                        | Strut | Free Surface | Total |
| 0                 | 1.67                      | 3.22  | -2.22        | +2.67 |
| 0.025             | 1.54                      | 2.60  | -2.18        | +1.96 |
| 0.05              | 1.42                      | 2.20  | -2.15        | +1.47 |
| 0.075             | 1.29                      | 1.85  | -2.11        | +1.03 |
| 0.10              | 1.16                      | 1.55  | -2.07        | +0.64 |
| 0.15              | 0.97                      | 1.17  | -2.00        | +0.14 |
| 0.20              | 0.81                      | 0.85  | -1.92        | -0.26 |
| 0.25              | 0.69                      | 0.67  | -1.85        | -0.49 |
| 0.30              | 0.58                      | 0.50  | -1.78        | -0.70 |
| 0.35              | 0.53                      | 0.37  | -1.70        | -0.80 |
| 0.40              | 0.43                      | 0.30  | -1.63        | -0.90 |
| 0.45              | 0.38                      | 0.22  | -1.55        | -0.95 |
| 0.50              | 0.32                      | 0.18  | -1.48        | -0.98 |
| 0.55              | 0.28                      | 0.12  | -1.41        | -1.01 |
| 0.60              | 0.25                      | 0.08  | -1.33        | -1.00 |
| 0.65              | 0.22                      | 0.05  | -1.26        | -0.99 |
| 0.70              | 0.19                      | 0     | -1.18        | -0.99 |
| 0.75              | 0.18                      | 0     | -1.11        | -0.93 |
| 0.80              | 0.18                      | 0     | -1.04        | -0.86 |
| 0.85              | 0.21                      | 0     | -0.96        | -0.75 |
| 0.90              | 0.30                      | 0     | -0.89        | -0.59 |
| 0.925             | 0.37                      | 0     | -0.85        | -0.48 |
| 0.95              | 0.46                      | 0     | -0.81        | -0.35 |
| 0.975             | 0.60                      | 0     | -0.78        | -0.18 |
| 1.000             | 0.78                      | 0     | -0.74        | +0.04 |



BuSHIPS PARENT FOIL



TAP-1



TAP-2

FIGURE 1A COMPARISON OF FOIL SECTIONS

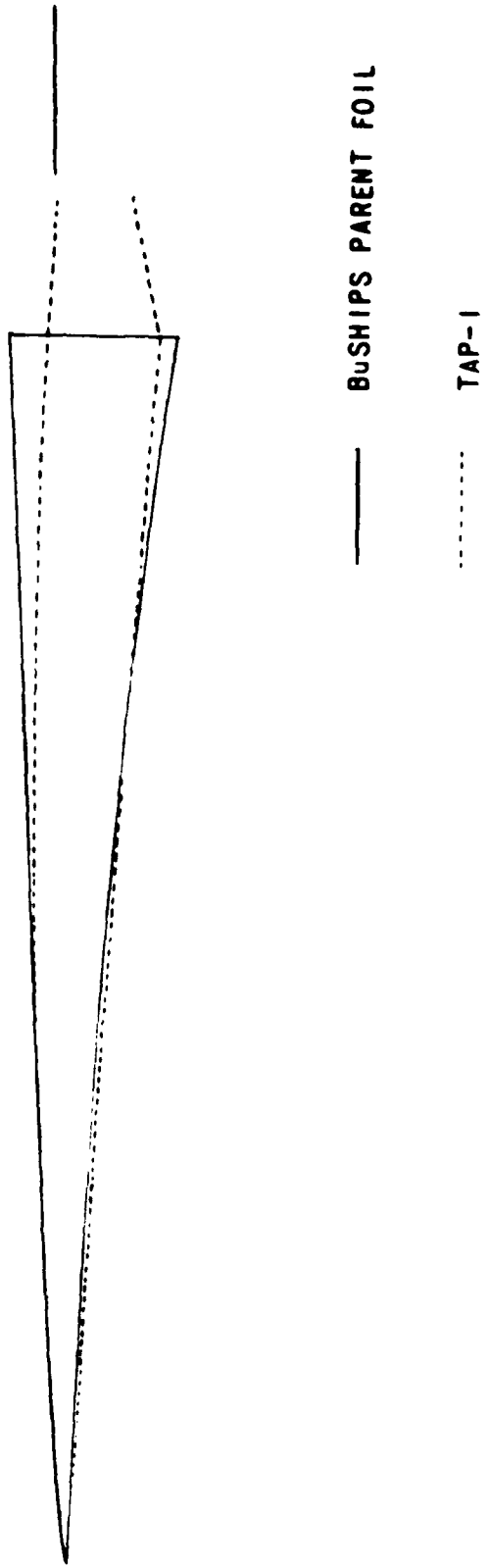


FIGURE 1B COMPARISON OF FOIL SECTIONS

BUSHIPS PARENT FOIL

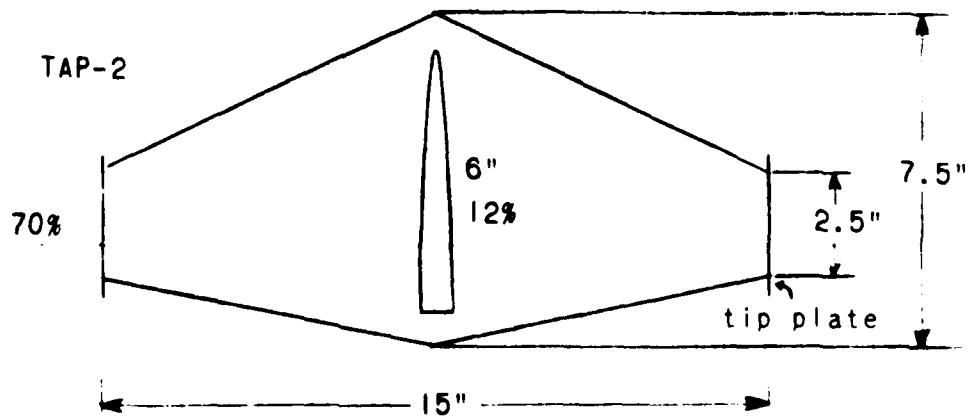
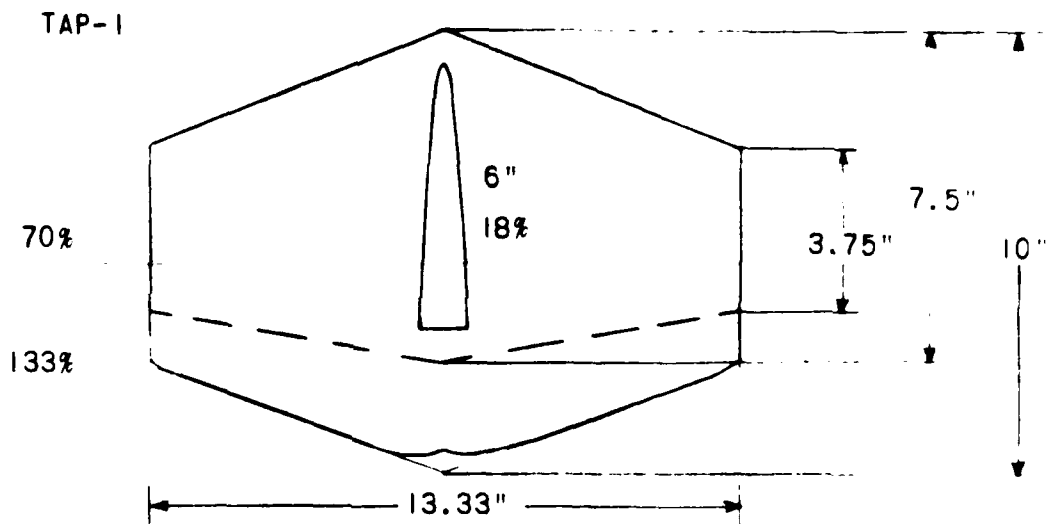
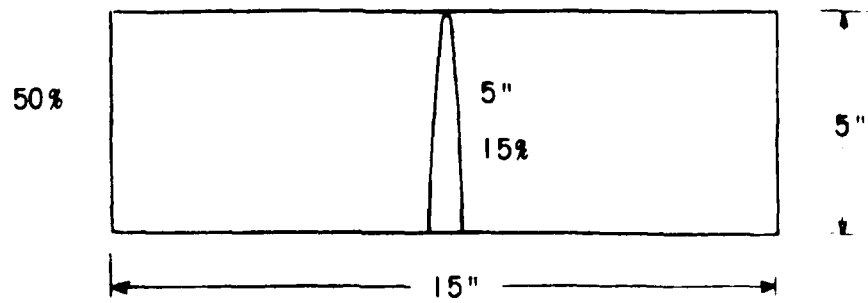


FIGURE 2 COMPARISON OF PLAN FORMS

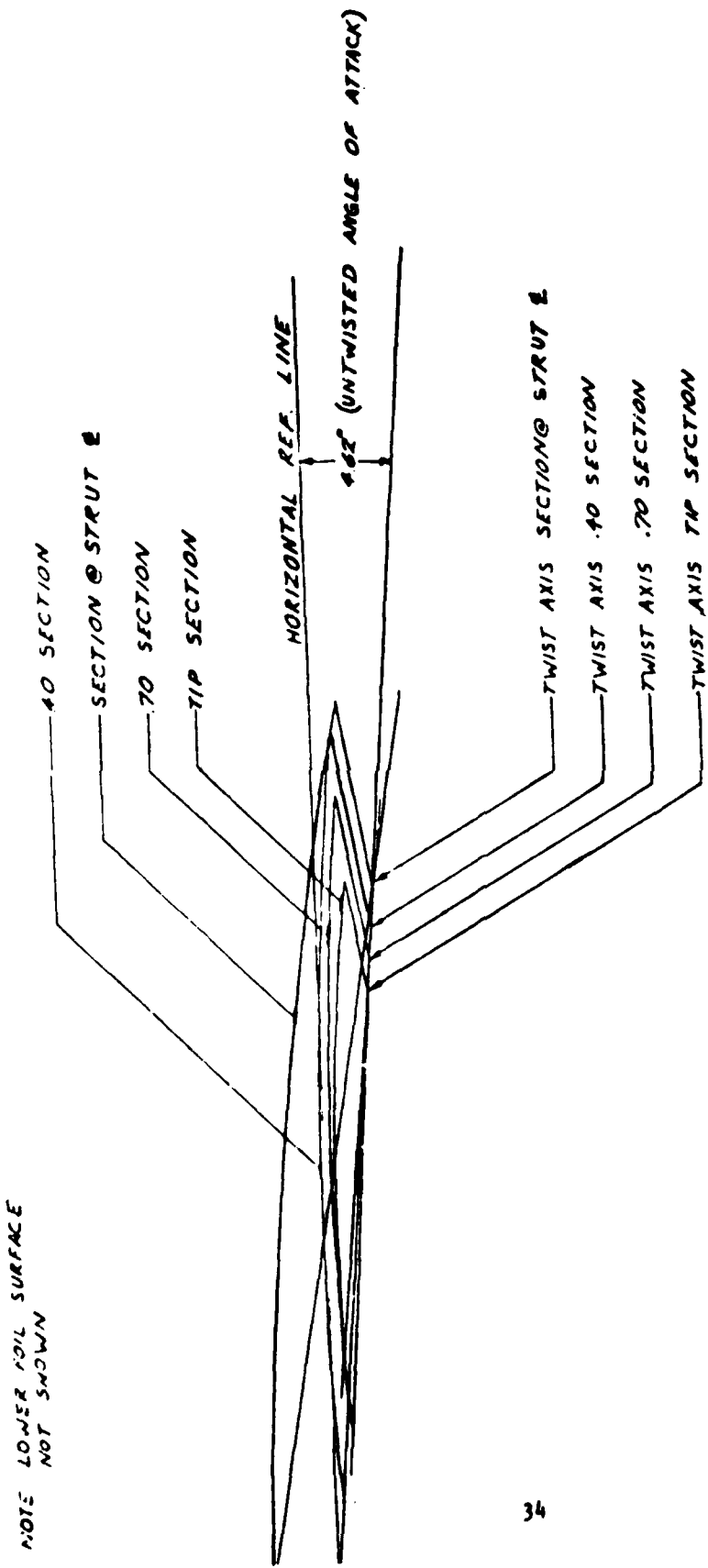


FIGURE 3 DEFINITION OF TWIST AXIS



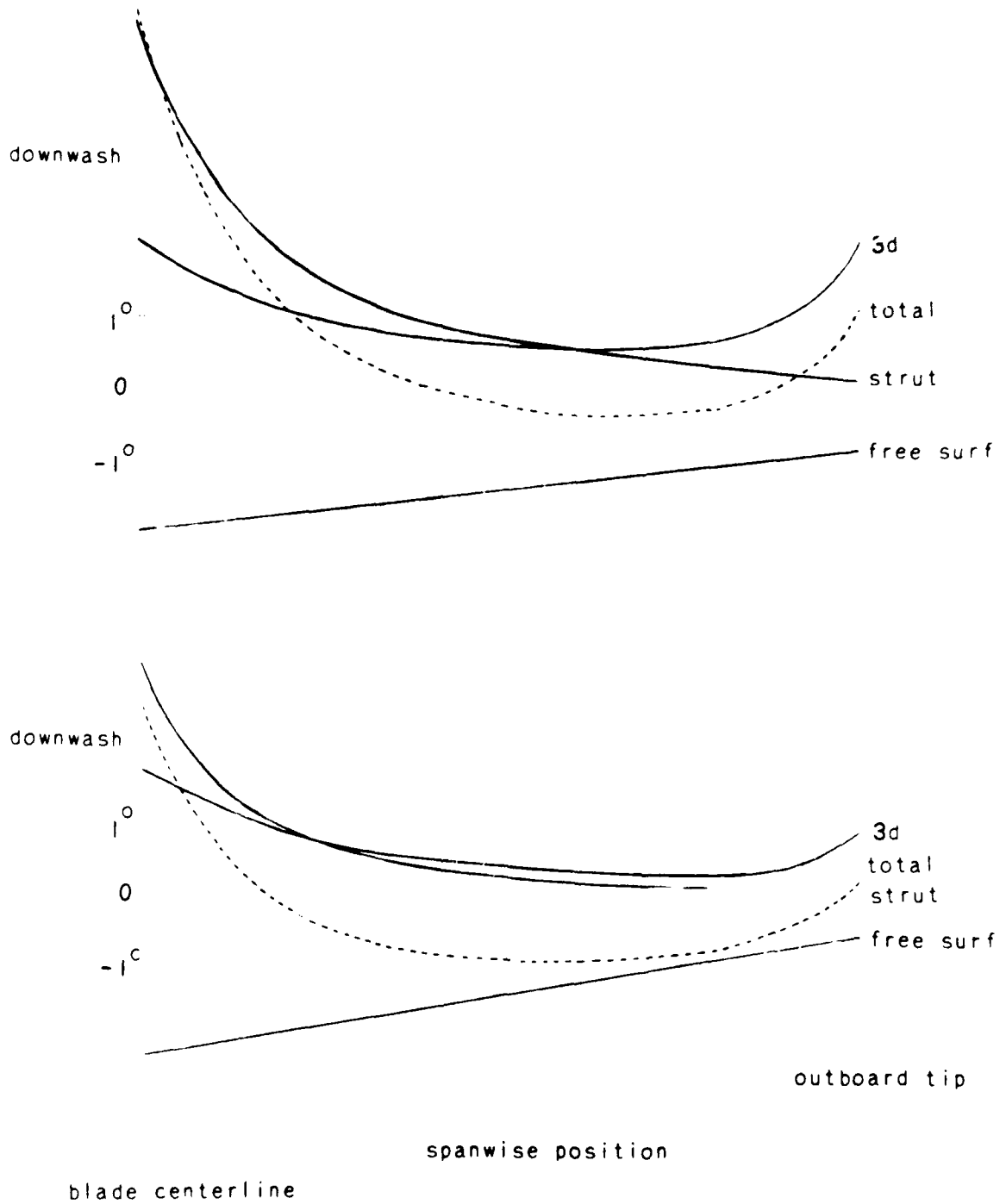


FIGURE 4 SPANWISE TWIST ANGLES

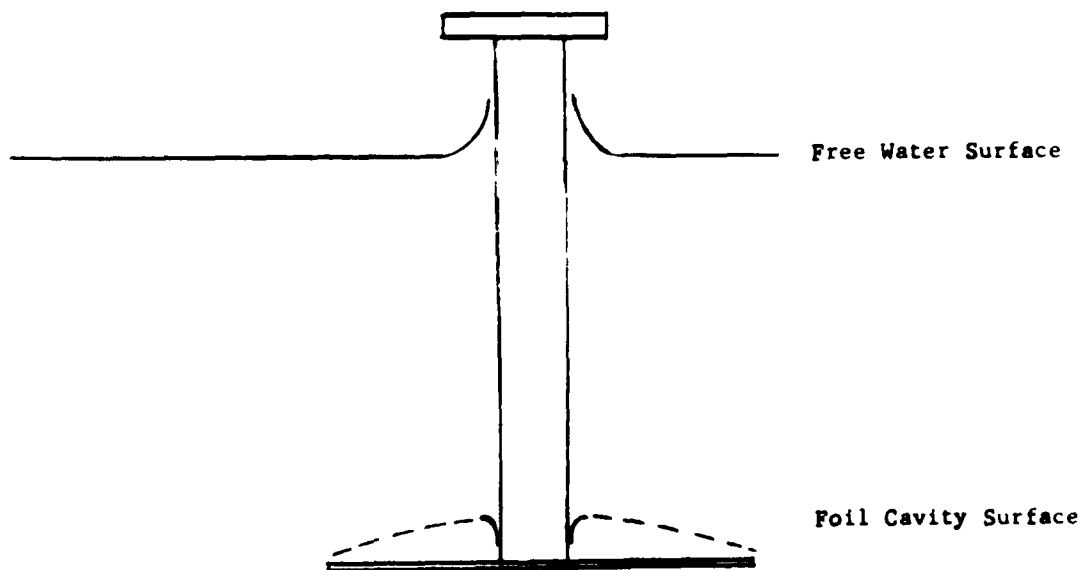
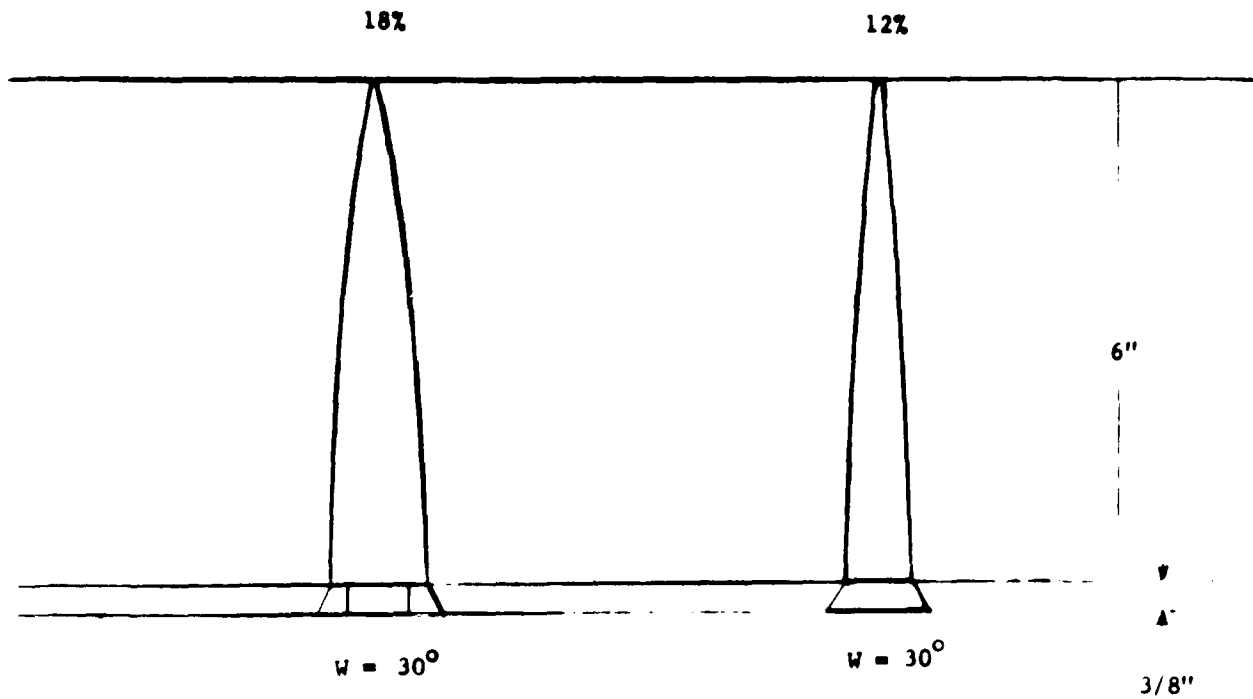


FIGURE 5 STRUT SPRAY WEDGES AND BOUNDARY LAYER

DISTRIBUTION LIST

NAVSHIPSYSCOM (SHIPS 03411)  
NAVSHIPSYSCOM (PMS 303)  
NAVSEC (SEC 6110)  
CIT (Acosta)  
Univ. of Mich. (Ogilvie)  
ARL (Parkin)  
Boeing Aerospace Company (Ray, Longfelder, Kiehle) (3 copies)  
Grumman Aircraft (Wright)

INTERNAL DISTRIBUTION

1150 (Johnston)  
1151 (O'Neill)  
1158 (Clark)  
15  
1509  
152  
1524 (Shen)  
1532 (Dobay)  
1532 (Baker) (5)  
1532 (Gregory)  
1532L (Holling)  
1532 (Moore)  
154  
1542  
1552  
1552 (Langan)  
1556  
1556 (Besch)  
1556 (Rood)  
1562  
1572  
1572 (Zarnick)  
1572 (Gersten)  
1576  
1731 (Buckley)  
1843 (Schott)

**DTNSRDC ISSUES THREE TYPES OF REPORTS**

(1) DTNSRDC REPORTS, A FORMAL SERIES PUBLISHING INFORMATION OF PERMANENT TECHNICAL VALUE, DESIGNATED BY A SERIAL REPORT NUMBER.

(2) DEPARTMENTAL REPORTS, A SEMIFORMAL SERIES, RECORDING INFORMATION OF A PRELIMINARY OR TEMPORARY NATURE, OR OF LIMITED INTEREST OR SIGNIFICANCE, CARRYING A DEPARTMENTAL ALPHANUMERIC IDENTIFICATION.

(3) TECHNICAL MEMORANDA, AN INFORMAL SERIES, USUALLY INTERNAL WORKING PAPERS OR DIRECT REPORTS TO SPONSORS, NUMBERED AS TM SERIES REPORTS; NOT FOR GENERAL DISTRIBUTION.